Nature of Interaction Between Basic Fibroblast Growth Factor and the Antiangiogenic Drug 7,7-(Carbonyl-bis[imino-*N*-Methyl-4,2-pyrrolecarbonylimino[*N*-methyl-4,2-pyrrole]-carbonylimino])-bis-(1,3-naphthalene disulfonate)

Moreno Zamai,*# Valeria R. Caiolfa,* Dina Pines,# Ehud Pines,# and Abraham H. Parola#
*Department of Oncology, Preclinical Research, Pharmacia & Upjohn, 20014 Nerviano, Milan, Italy, and #Department of Chemistry, Ben-Gurion University of the Negev, 84 105 Beer-Sheva, Israel

ABSTRACT PNU145156E (7,7-(carbonyl-bis[imino-*N*-methyl-4,2-pyrrolecarbonylimino[*N*-methyl-4,2-pyrrole]-carbonylimino])-bis-(1,3-naphthalene disulfonate)) is a naphthalene sulfonic distamycin A derivative that interacts with heparin-binding growth factors. Because PNU145156E inhibits tumor angiogenesis, it was selected for clinical development. Picosecond time-resolved fluorescence emission and anisotropy were used to characterize the binding of PNU145156E to the basic fibroblast growth factor (a protein associated with tumor angiogenesis). A decrease in PNU145156E fluorescence lifetime was observed as a function of human basic fibroblast growth factor (bFGF) concentration. Nonlinear least-squares fitting of the binding isotherm yielded K_d = 145 nM for a single class of binding sites. Time-resolved anisotropy gave K_d = 174 nM. K_d = 150 nM was independently verified by quantitative high-performance affinity chromatography. The displaced volume of the complex, calculated from its rotational correlation time, fitted a sphere of 1:1 stoichiometry. These results account for the formation of a tight yet reversible PNU145156E:bFGF complex. An evaluation of PNU145156E fluorescence lifetimes in various solvents has highlighted the forces involved in stabilizing the complex. These are mostly electrostatic-hydrophobic in nature, with a relatively low contribution from hydrogen bonding. Both polar and nonpolar groups are involved on the protein-binding site within a largely hydrophobic cleft. A potential binding trajectory, based on a combination of these results with site-directed chemical modification and known bFGF x-ray structure, is suggested.

INTRODUCTION

Angiogenesis results from a series of molecular events that are regulated by stimulators and inhibitors (Klagsbrun and D'Amore, 1991). This process is fundamental in the development of a series of pathologies, such as solid tumor growth and metastatic spread (Folkman, 1971, 1985). Since the demonstration of the role of angiogenesis in cancer, the sequential steps involved in tumor angiogenesis have been partially elucidated. Thus the search for angiogenesis inhibitors has become the focus of several research groups. A variety of tumor-induced angiogenesis factors have been identified and are known to have a widespread effect on different steps of angiogenesis. They play a role in tumor progression and metastasis through a direct stimulus to cell division and/or through activation of neovascularization (Gullino, 1978; Folkman and Klagsbrun, 1987; Blood and Zetter, 1990; Liotta et al., 1991).

An important class of angiogenesis-promoting proteins is the heparin-binding growth factors. Its archetypal member, human basic fibroblast growth factor (bFGF), is involved in solid tumor development (Burgess and Maciag, 1989; Basilico and Moscatelli, 1992; Presta et al., 1994). bFGF is associated with the extracellular matrix and basement membrane of endothelial cells, where it is stored and from which it is released when the extracellular matrix is degraded (Vlodavsky et al., 1991). A specific structure of heparin and heparan sulfate proteoglycans is required for bFGF storage and for productive binding of bFGF to its receptor (Klagsbrun and Baird, 1991; Fernig and Gallagher, 1994; Lindahl et al., 1994; Ornitz et al., 1995; Faham et al., 1996). Chemical and site-directed mutagenesis studies on bFGF, supported by x-ray crystallography, have identified separated functional domains for heparin and for receptor binding (Baird et al., 1988; Zhu et al., 1990; Eriksson et al., 1993; Thompson et al., 1994; Springer et al., 1994; Zhu et al., 1995).

The possible modulation of tumor progression by drugs that inhibit angiogenic factors is an intriguing approach, representing a new concept in adjuvant anticancer chemotherapy (Herblin et al., 1994; Auerbach and Auerbach, 1994). In the last few years, naphthalene sulfonic distamycin A derivatives were shown to inhibit the binding of human recombinant bFGF to its receptors, to block in vivo bFGF-induced vascularization, and to stop neovascularization in chorioallantoic membrane (Ciomei et al., 1993). In particular, PNU145156E was shown to inhibit the growth of murine tumors in vivo and to have a rather low toxicity (Sola et al., 1995). These compounds are polysulfonated naphthylureas structurally related to suramin, which is currently being investigated as an antitumor agent for the treatment of advanced malignancies (La Rocca et al., 1990; Kohler et al., 1992). Suramin causes a nonspecific and irreversible protein aggregation (Middaugh et al., 1992).

Received for publication 20 October 1997 and in final form 21 April 1998.
Address reprint requests to Dr. Abraham H. Parola, Department of Chemistry, Ben Gurion University of the Negev, P.O. Box 653, Beer-Sheva 84105, Israel. Tel.: +972-7-6472454, +972-7-6461188. Fax: +972-7-6472943. E-mail: aparola@bgumail.bgu.ac.il.

0006-3495/98/08/672/11 $2.00

Unlike suramin, the mechanism of action of naphthalene sulfonic distamycin A derivatives is suggested to involve direct binding to the growth factor (Biasoli et al., 1993; Zamai et al., 1997).

Our present goal is to define the stoichiometry of the bFGF-drug complex and to understand the nature of the forces involved in this interaction. As a representative molecule, we have chosen PNU145156E (7,7-(carbonyl-bis [imino-*N*-methyl-4,2-pyrrolecarbonyl-imino(*N*-methyl-4,2-pyrrole)carbonylimino]-bis-(1,3-naphthalene disulfonate) (Scheme 1), which is the lead compound currently under clinical trial.

The complex between bFGF and PNU145156E was not yet crystallized. Accordingly, the x-ray structure of the complex is hitherto unavailable. At the high concentration required for crystallization of this complex, self-aggregation of PNU145156E takes place. Alternatively, photon counting spectrofluorimetry provides a sensitive analytical tool for the study of the nature of the interaction between bFGF and PNU145156E at concentrations close to the physiological range at which self-aggregation does not occur.

We have studied by picosecond single-photon correlation spectroscopy the fluorescence emission and anisotropy decay profiles of PNU145156E as a function of recombinant human bFGF concentration. The measurements were carried out in an in vitro cell-free system. Because of the low quantum yield of the drug, the single-photon counting apparatus was optimized for high detection sensitivity. The lowest concentration of the drug analyzed was 10 nM. This sensitivity is comparable to that of 0.1 nM of typical dye molecules. Binding stoichiometry and reversibility were then assessed. The affinity of the drug to bFGF was also verified by high-performance quantitative affinity chromatography. The solvent effect on the PNU145156E lifetime was evaluated to decipher the forces involved in the drug-protein interaction. The solvent effect was used to model the various binding interactions in the complex. Binding affinities for native and carboxymethylated bFGF were compared.

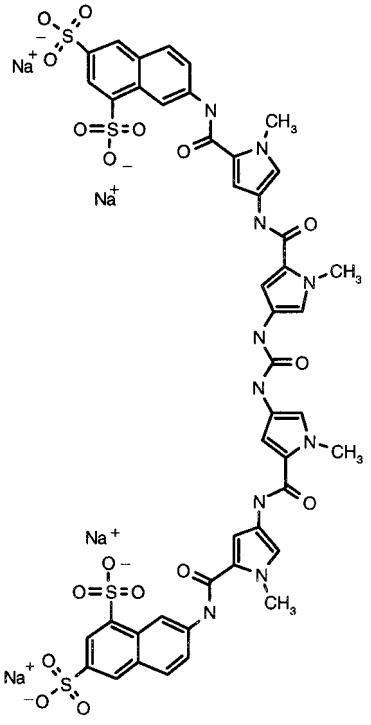

Scheme 1.

MATERIALS AND METHODS

Reagents and solutions

PNU145156E (MW 1273; 98% purity assessed by elemental analysis and NMR) was synthesized by Pharmacia & Upjohn. Human recombinant fibroblast growth factor (bFGF) was produced by Pharmacia & Upjohn or was obtained from PeproTech (Rocky Hill, NJ). The carboxymethylated form of bFGF (Cm-FGF) was a gift of Dr. P. Caccia (Caccia et al., 1992). Both proteins were checked by sodium dodecyl sulfate polyacrylamide gel electrophoresis. A single band of 17,000 MW was detected for both proteins. Na_2HPO_4, NaH_2PO_4, NaCl, $NaHCO_3$, ethanolamine, sodium acetate, and high-performance liquid chromatography (HPLC)-grade water were purchased from Carlo Erba Reagents (Milan, Italy). Anhydrous and spectroscopic grade 1,4-dioxane, methanol, isopropanol, and acetonitrile were obtained from Sigma (St. Louis, MO) and Aldrich (Milwaukee, WI). Accell, *N*-hydroxysuccinimide ester activated affinity support, was obtained from Waters (Milford, MA). HPLC glass columns for packing affinity matrices were obtained from Omnifit (Atlantic Beach, NY). All of the solutions were filtered through 0.22-μm filters before use. Phosphate-buffered saline (PBS) containing 7.5 mM NaH_2PO_4, 17.5 mM Na_2HPO_4, 0.15 M NaCl (pH 7.1) was used in affinity chromatography. Fluorescence binding experiments were run in 6 mM NaH_2PO_4, 14 mM Na_2HPO_4, 0.15 M NaCl (pH 7.1). For bFGF immobilization the following buffers were used: coupling buffer containing 0.2 M $NaHCO_3$, 0.5 M NaCl (pH 8.3); end-capping buffer containing 0.5 M ethanolamine, 0.2 M $NaHCO_3$, 0.5 M NaCl (pH 8.3); and washing buffer containing 0.1 M sodium acetate, 0.5 M NaCl (pH 4.0).

Steady-state fluorescence anisotropy

Steady-state fluorescence anisotropy (Hazan et al., 1995; Alfahel et al., 1996) was studied in PBS (pH 7.2) at 22°C. The experiments were carried out on a computer-controlled Perkin-Elmer LS50 spectrofluorimeter (Milford, CT) equipped with polarizers and a LKB2219 Multitemp II thermostatic circulator ($\pm$0.1°C, Stokholm, Sweden). Anisotropy was measured in the L-format at λ_{ex} = 360 nm/λ_{em} = 450 nm. Under these conditions, total sample absorptivity was lower or equal to 0.2 O.D., avoiding inner filter or scattering effects. Slits were set at 4.5 nm in excitation and 20 nm in emission (Zamai et al., 1997). The *G* factor was determined for correction. Data were collected and elaborated by the FLDM Perkin-Elmer anisotropy obey routine. This technique was used to study the titration of PNU145156E (2.85 μM) by bFGF and Cm-FGF (bFGF carboxymethylated at Cys^{69} and Cys^{87}).

Single-photon counting setup

The single-photon counting setup was based on a Spectra Physics Ti-sapphire Tsunnami laser (Mountain View, CA), which was pumped by a BeamLok Spectra Physics 10-W argon ion laser and produced a pulse train of 1 ps duration at a repetition rate of 82 MHz. The Ti-sapphire laser was run with Spectra Physics "blue" optics and was tuned between 690 and 800 nm. The fundamental frequency was pulse picked by a Spectra Physics model 3980 apparatus so as to reduce the fundamental pulsed frequency to 4 or 0.8 MHz. The picked pulses were then passed through a Spectra Physics frequency doubler to produce the desired excitation wavelength (typically 350–365 nm). The single-photon counting detection system was

run at the reversed timing mode and was based on Tennelek and Ortec state-of-the-art nim-bin components. To minimize the time uncertainty associated with the single-photon counting time correlation technique, we used a Hamamatsu 3809u 6 μ multichannel plate as the light detector. Wavelength selection was achieved by passing the incoming light through a double monochromator (CVI, CM112, 1/8 meter; Laser Corporation, Albuquerque, NM), which was used in its subtractive mode. The full width at half-maximum (FWHM) of the instrument response was typically 25 ps, with a best achieved response of 17 ps. The resolution of this setup after data processing was typically 2–5 ps, depending on the time range of the time-to-amplitude converter (TAC) Tennelek 862 (Oak Ridge, TN). In this respect, our setup presents the best performance ever achieved. Anisotropy measurements were conducted by ensuring the horizontal polarization of the laser beam by means of a Glan prism. The polarized light was then passed through a Berek's polarization compensator (New Focus, Sunnyvale, CA), which acts like a variable waveplate. This enabled us to rotate the polarization of the excitation beam while fixing the polarization of the light entering the double monochromator at vertical polarization. This configuration avoided complication due to the large G factor of the double monochromator. Temperature was kept constant at 20°C with a thermostatted cell holder that was stabilized to better than $\pm$0.05°C by a Neslab (Portsmouth, NH) chiller.

Time-resolved fluorescence measurements

Experiments were carried out with a total sample absorptivity either lower than or equal to 0.2 optical density units (O.D.), so as to avoid inner filter effects and to ensure linearity across the optical path of a 1-cm cuvette. Samples were excited at 360 nm, the excitation maximum, and their emission was collected at 440 nm. PNU145156E fluorescence emission was sampled for 360 s for parallel, perpendicular, and the magic angle relative orientation between the excitation and emission polarizers (New Focus). The minimum number of photons, 2–5 K in the peak channel, was obtained by proper adjustment of neutral density filters. Decay profiles were obtained at a resolution of 12.5 ps/channel at 20°C. Control background fluorescence was obtained from samples containing no drug. Data analyses were performed by noncommercial software. Time-resolved emission spectral data were fitted to a discrete lifetime model. The fluorescence decayed according to a double exponential decay. Fluorescence anisotropy parallel and perpendicular decay components were analyzed according to a model based either on a single or on a double exponential for both the free drug and its complex with bFGF. Data processing was done by the ISS Global analysis program (ISS, Champagne, IL). Other models, e.g., a triple exponential decay for the complex, resulted in less favorable χ^2.

Determination of dissociation constants

Fluorescence lifetime titration was used to determine the dissociation constant, K_d, of the PNU145156E:bFGF complex (Burke and Mi, 1994). The concentration of PNU145156E was kept constant and equal to 0.31 μM in PBS (pH 7.1), and the lifetime was measured at increasing bFGF concentrations. In control runs, PNU145156E was substituted by buffer. The model of simple bimolecular association with ligand depletion was applied to the experimental lifetimes, τ, measured as a function of bFGF concentration, [P] (Hulme and Birdsall, 1992):

$$A = (A_{min} - (A_{min} - A_{max})/2[D]) \cdot (([P] + [D] + K_d) - (([P] + [D] + K_d)^2 - 4[D] \cdot [P])^{1/2}) \quad (1)$$

where A is τ, and A_{min} and A_{max} are the lifetime values of free (τ_F) and bound (τ_B) drug, respectively. [D] is the PNU145156E molar concentration. K_d was determined from Eq. 1. The contribution of protein to the total intensity was less than 3%.

PNU145156E titration by bFGF was also followed by polarized excitation. Because of the low fluorescence intensity of the drug, 2.15 μM PNU145156E was required in these experiments. The dissociation constant K_d was determined by applying Eq. 1 to rotational correlation time, ϕ, as a function of the molar concentration of bFGF, [P]. In this case, A is ϕ; A_{min} and A_{max} are the rotational correlation time values of free (ϕ_F) and bound (ϕ_B) drug. The contribution of protein to the total intensity was less than 2%.

All fittings were obtained by nonlinear least-squares regression, using Prism2 (GraphPad, San Diego, CA), applying a convergence criterion by which two consecutive iterations reduced the sum of squares by less than 0.01%.

Preparation of high-performance affinity columns

Immobilization of human recombinant bFGF to Accell matrix was carried out, following a procedure described previously (Zamai and Fassina, 1991). Briefly, 6 mg of bFGF was dissolved in 8 ml of coupling buffer and incubated with 0.6 g of matrix, for 4–8 h under agitation at 4°C. The reacted matrix was incubated twice with 20 ml of end-capping buffer for 2 h at room temperature and washed twice with 20 ml of washing buffer. This washing was repeated twice with 20 ml of coupling buffer and three times with 20 ml of HPLC-grade water. A blank matrix was prepared by reacting 1 g of Accell with 20 ml of end-capped buffer, for 2 h at room temperature, followed by washing as before.

Quantitative high-performance affinity chromatography

The bFGF-matrix was packed into a 100 $\times$ 3 mm inner diameter Omnifit HPLC glass column. The column was connected to a Pharmacia-LKB HPLC gradient pump 2249 equipped with a Milton Roy SM4000 programmable wavelength detector and a Merck-Hitachi D-2500 Chromato-Integrator. Binding to immobilized bFGF, at 22°C, was followed by continuous (broad zone) elution of PNU145156E at different concentrations. Accordingly, the immobilized-bFGF column was equilibrated with PBS elution buffer at a flow rate of 1 ml/min. Then each concentration of PNU145156E in PBS was continuously eluted through the affinity column and monitored by UV absorbance at 320 nm, until a plateau of maximum absorbance was observed. Elution volumes were determined by frontal analysis as V, the volume at half-maximum absorbance in the sigmoid elution front. V was corrected for a small shoulder (3% by mass) of UV-absorbing noninteracting material observed at the void volume V_0. The variation in elution volume V was evaluated by the equation

$$1/(V - V_0) = K_d/M_T + [L]_0/M_T \quad (2)$$

where V is the volume at which the affinity matrix is half-saturated by the ligand, V_0 is the void volume, K_d is the dissociation constant of the bFGF:PNU145156E complex, M_T is moles of immobilized bFGF at saturation, and $[L]_0$ is the initial concentration of the mobile ligand PNU145156E (in the broad elution zone, initial and plateau values of [L] are identical) (Fassina and Chaiken, 1987). The intercept of $1/(V - V_0)$ versus $[L]_0$ yielded K_d values (*inset* in Fig. 5).

Solvent effect on the fluorescence lifetime of PNU145156E

PNU145156E fluorescence lifetime decay was studied in various solvents to characterize the solvation effect. It is common in such a case to use empirical solvent parameter analyses that take into account all nonspecific and specific local solute/solvent interactions. The photophysical indicator chosen to correlate with the empirical solvent parameters was the relative quantum yield of the long lifetime component of PNU145156E fluorescence, normalized to the amplitude of the lifetime in H_2O (i.e., $\bar{\tau} = \tau_2\alpha_2/\alpha_2^{H2O}$). $\bar{\tau}$ values were fitted using either a single-parameter or multiparameter approach. In the single-parameter analysis, correlation with Kosower's Z value (Kosower, 1968) or with Ditmar and Reinchardt's E_T^{30} value (Reichardt, 1990, 1994) was considered. Z values represent solvent

polarity based on UV absorption spectra of a charge-transfer molecule. E_T^{30} values represent a combined measure of solvent dipolarity/polarizability and solvent hydrogen bond donor activity. In the present case, we used $E_T^N(30)$ (i.e., E_T^{30} normalized by using water and tetramethylsilane (TMS) as extreme reference solvents; Reichardt, 1990). In the multiparameter treatment, Krigowski and Fawcett's procedure (Krygowski and Fawcett, 1975; Glikberg and Marcus, 1983; Zhong-yuan et al., 1985), based on Ditmar and Reichardt's E_T^{30} and Gutmann's donor number (DN) (Gutmann, 1968), was used. The following equation was applied:

$$\bar{\tau} = P(1)E_T^N(30) + P(2)\mathrm{DN} + P(3) \quad (3)$$

where $E_T^N(30)$ are E_T^{30} values normalized to a strong donor solvent (hexamethyl phosphoric triamide (HMPT); Reichardt, 1990). They were chosen as a measure of Lewis acidity. Gutmann's donor number values, DN, were chosen as a measure of solvent basicity. $P(1)$ and $P(2)$ are regression coefficients describing the sensitivity of normalized lifetime to electrophilic and nucleophilic solvent properties. $P(3)$ is a constant obtained by the regression. We have also explored the multiparameter approach proposed by Taft (Abraham et al., 1988, and references therein). In this approach each solvent is characterized by a set of parameters that are thought to be orthogonal to each other. The advantage is in the possibility of identifying and isolating each type of solvent interaction. The property under investigation in a set of solvents can be expressed as

$$\bar{\tau} = A_0 + s(\pi^* + d\delta) + a\alpha + b\beta \quad (4)$$

where A_0, a, b, d, and s are regression constants; π^*, nonspecific solute/solvent interactions, measures the ability of the solvent to stabilize a charge or a dipole; α is the solvent hydrogen bond donor acidity; and β is the solvent hydrogen bond acceptor basicity. The δ parameter is a "polarizability correction term" equal to zero for nonchlorinated aliphatic solvents.

RESULTS

Characterization of PNU145156E:bFGF complex by following fluorescence lifetime and anisotropy decays

Time-resolved fluorescence decay profiles of PNU145156E (0.31 μM) were obtained by following fluorescence emission at 440 nm upon excitation at 360 nm in PBS (pH 7.1) at 20°C. Fig. 1 *A* depicts the fluorescence decay profile of free PNU145156E in buffer, and Fig. 1 *B* shows the fluorescence decay profile of the drug in the presence of 3.96 μM of bFGF. For the free, unbound drug, the best double-exponential fit resulted in a short component, $\tau_1 = 0.6$ ns, and a long component, $\tau_2 = 10.7$ ns, and amplitudes $\alpha_1 = 0.76$ and $\alpha_2 = 0.24$, respectively. The long component, which carries most of the fluorescence quantum yield, was found to be both environmentally sensitive and reproducible. The bound drug showed a remarkable decrease of the long component, $\tau_2 = 6.8$ ns, with no change in τ_1. Relative amplitudes also changed considerably to $\alpha_1 = 0.96$ and $\alpha_2 = 0.04$ (in all cases, χ^2 of the fitted data ranged between 1.05 and 1.51). Distributional analyses (not shown) with one or two Lorentzian distributions did not improve the quality of the two-exponential lifetime fit. A plot of τ_2, as a function of bFGF concentration, is shown in Fig. 2. At bFGF concentrations corresponding to the plateau range of Fig. 2, a 36% decrease in τ_2 was observed. The best nonlinear least-squares fit of τ_2 values was found to follow Eq. 1 (see Materials and Methods). The dissociation constant

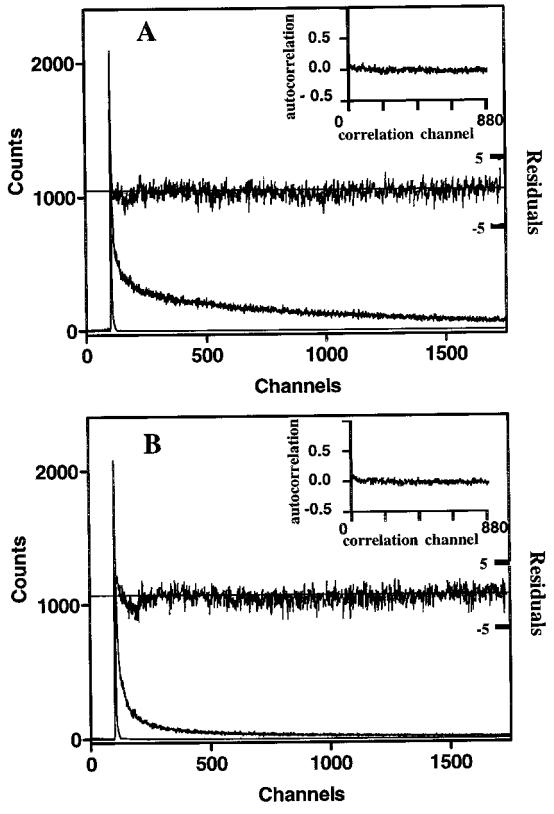

FIGURE 1 Fluorescence emission decays of (*A*) free and (*B*) bFGF-bound PNU145156E in PBS (pH 7.1) at 20°C. [PNU145156E] = 0.31 μM and [bFGF] = 3.96 μM. (*Insets*) Autocorrelation functions and residuals. The instrumental lamp function is shown in each case. Calibration: 12.5 ps/channel; λ_{ex}max = 360 nm; λ_{em}max = 440 nm. Time-resolved emission spectral data were deconvoluted according to the discrete decay model.

(K_d) of the PNU145156E:bFGF complex, obtained by Eq. 1, was 145 ± 5 nM. This corresponds to a free energy of interaction $\Delta G = -38.4 \pm 1.3$ kJ mol^{-1}. We have also taken into account the changes in the relative amplitudes, associated with τ_1 and τ_2, using Eq. 1 as a basis for analyses of the weighted mean lifetime values ($\tau_{mean} = \tau_1\alpha_1 + \tau_2\alpha_2$, Table 1). In this case a dissociation constant of 134 ± 3 nM was obtained ($\Delta G = -38.6 \pm 0.9$ kJ mol^{-1}). The fluorescence lifetime of the free drug ($\tau_F = 10.75$ ns) was determined by the fitting. The fitted value agrees with our experimental one (measured in the absence of protein). The value of the fluorescence lifetime of the fully bound drug ($\tau_B = 6.82$ ns) was determined by extrapolating to infinite protein concentration. For both analyses (τ_2 and τ_{mean}), the linearity of Scatchard plots approximates a single mode of binding (*inset* in Fig. 2). The agreement between the two analyses indicates that the long lifetime component is the most sensitive parameter in the interaction between the drug and bFGF (Table 1). In addition, a dilution experiment was performed. The PNU145156E fluorescence lifetime was measured to be 6.94 ns in a solution with a bFGF/PNU145156E ratio of 15.5. This sample was gradually diluted to bFGF/PNU145156E ratios of 7.7 and 2.54 by

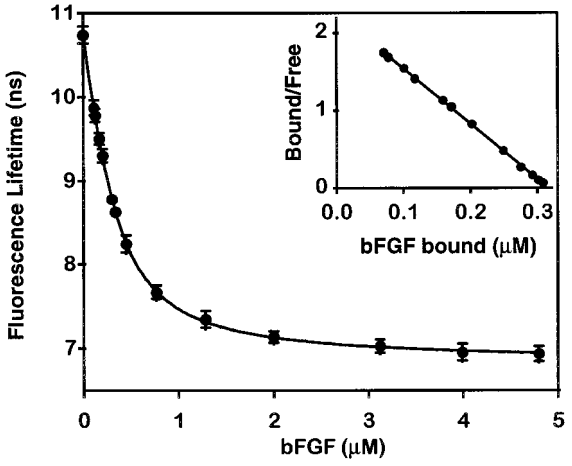

FIGURE 2 Binding of PNU145156E to bFGF, in PBS (pH 7.1) at 20°C, as monitored by fluorescence lifetime titration. The fluorophore concentration was 0.31 μM, and the bFGF concentration was varied from 0.1 μM to 4.9 μM. The variation of the long lifetime component τ_2 is plotted versus bFGF concentration. The best nonlinear least-squares fit is represented by the solid line. The average of duplicate runs is shown, and each point has a variance of 4% or less. (*Inset*) Scatchard plot.

adding a 0.31 μM solution of PNU145156E. The fluorescence lifetime went up to 7.10 ns and to 7.62 ns, respectively. These two data points fall on the fitted curve in Fig. 2. The result indicates the reversibility of the complex interaction.

Fig. 3 shows the dependence of PNU145156E fluorescence anisotropy on complex formation between bFGF and PNU145156E. Time-resolved anisotropy decays of PNU145156E (2.15 μM in PBS, pH 7.1, at 20°C), in the absence and in the presence of bFGF (9.79 μM), were compared (Fig. 3, *A* and *B*, respectively). PNU145156E displayed a rapid anisotropy decay that was deconvoluted, when we used either a single- or a double-exponential function (Fig. 3 *A*). The global fit to a single-exponential function gave an averaged rotational correlation time ϕ of 0.08 ns with a χ^2 value of 1.31 (Table 1). The double-exponential fit yielded a ϕ_1 of 0.025 ns ($\alpha_1 = 0.8$) and a ϕ_2 of 0.300 ns ($\alpha_2 = 0.2$) with a χ^2 value of 1.21. The presence of two rotational correlation times can be explained by the rodlike structure of PNU145156E (Scheme 1) rotating around two different axes. In the presence of bFGF, the results of anisotropy decay changed remarkably (Fig. 3 *B*). A dose response increase in PNU145156E averaged rotational correlation time ϕ (χ^2 always <1.6) was detected on titration with bFGF (Fig. 4). The best nonlinear least-squares analysis of ϕ (*solid line* in Fig. 4) was obtained by applying Eq. 1. The dissociation constant (K_d) of the complex was 174 $\pm$ 4 nM with a free energy of interaction $\Delta G = -37.9 \pm 0.9$ kJ mol^{-1}. The rotational correlation time of the free drug (ϕ_F), obtained with Eq. 1, is again in agreement with the averaged rotational correlation time, $\phi = 0.08$ ns, measured in the absence of bFGF. The rotational correlation time of the bound drug, $\phi_B = 6.56$ ns, was therefore determined by extrapolation to infinite bFGF molar concentration in Eq. 1. In this case, too, the Scatchard plot was linear (Fig. 4, *inset*).

PNU145156E and bFGF interaction detected and quantified by QHPAC

To substantiate the results obtained by time-resolved fluorescence, the interaction between PNU145156E and bFGF was also studied by Quantitative high-performance affinity chromatography (QHPAC). This is a technique based on affinity chromatography. Buffer solutions (PBS at pH 7.1) of the ligand are eluted in a bFGF column, according to the continuous elution method (see Materials and Methods). Elution profiles at room temperature of increasing concentrations of the drug (mobile phase) throughout a 100 $\times$ 3 mm bFGF-column (stationary phase) are shown, overlaid, in Fig. 5. Their frontal analysis enabled us to quantify the affinity of PNU145156E for immobilized bFGF (Eq. 2, *inset* in Fig. 5). In the presence of a total immobilized amount of bFGF (M_T) = 2.7 $\pm$ 0.1 nmol, the dissociation constant for the complex was $K_d = 150 \pm 7$ nM. This value corresponds to a free energy of interaction $\Delta G = -38.3 \pm 1.8$ kJ mol^{-1} (Table 1). QHPAC also reveals the presence of some UV-absorbing, noninteracting material that elutes at the void V_0. This material elutes as a shoulder of the drug profile and accounts for $\sim$3% of the total absorbance (Fig. 5). In this way, we could estimate 97% purity of PNU145156E stock, which accords well with the 98% value ascertained by traditional analyses (see Materials and Methods).

PNU145156E fluorescence lifetime in various solvents

To characterize the nature of the forces involved in the interaction between PNU145156E and bFGF, the effect of solvation on PNU145156E was studied by following its fluorescence lifetime decays. PNU145156E fluorescence lifetime values, in several solvents, are summarized in Table 2. Evidently, the fluorescence lifetime of the drug is strongly affected by the chemical nature of the solvent. This solvent effect cannot be described quantitatively by a single physical macroscopic solvent parameter such as the dielectric constant, refractive index, or functions thereof. It is quite common in such a case to use empirical solvent parameters to characterize the solvation effect of each solvent (Gutmann, 1968; Kosower, 1968; Krygowski and Fawcett, 1975; Glikberg and Marcus, 1983; Zhong-yuan et al., 1985; Abraham et al., 1988, and references therein; Reichardt, 1990, 1994). The use of empirical solvent parameters has the advantage of taking into account specific local solvation effects, such as hydrogen bonding and direct Lewis-type acid-base interactions. The resultant solvent effect analyses serve as a direct measure of the change in the environment of the drug (fluorophore).

TABLE 1 PNU145156E:bFGF dissociation constants determined by fluorescence and chromatography

Method	PNU145156E concentration (μM)	Elution volumes (ml)		Fluorescence decay times (ns)		K_d (nM)	ΔG (kJ)
Lifetime				τ_F	τ_B		
Decay titration	0.31			10.74	6.82	145 ± 5	−38.4 ± 1.3
Anisotropy				ϕ_F	ϕ_B		
Decay titration	2.15			0.08	6.56	174 ± 4	−37.9 ± 0.9
	Variable	V_o	V				
QHPAC	0.410–1.058	0.80	3.14			150 ± 10	−38.3 ± 1.8

The relative quantum yield of the long lifetime component of PNU145156E fluorescence, normalized to the amplitude of lifetime in H_2O ($\bar{\tau} = \tau_2\alpha_2/\alpha_2^{H_2O}$), was chosen to be correlated with the empirical solvent parameters (Table 2). This procedure resulted in a better correlation than when performed with either total quantum yield of fluorescence ($\alpha_1\tau_1 + \alpha_2\tau_2$) or simply τ_2 lifetime. In fact, both amplitude and lifetime were found to be solvent sensitive. $\bar{\tau}$ was measured in different solvents and was correlated with Kosower's Z value or with Ditmar and Reichardt's $E_T^N(30)$ value. We found these two correlations to be less successful (with $R = 0.850$ and $R = 0.946$, respectively) than multiparameter analysis. Furthermore, these fits (not shown) suffer from a calculated negative value for the dioxane data point. A better correlation was found by applying Krigowski and Fawcett's procedure, which uses $E_T^N(30)$ values, and Gutmann's donor number (DN) values. Fig. 6 *A* shows the correlation between $\bar{\tau}$ and $E_T^N(30)$ and DN, resulting in

$$\bar{\tau} = 22.24E_T^N(30) - 4.69\text{DN} - 6.65$$

with a correlation coefficient $R = 0.988$. The relative values of the coefficients indicate that $E_T^N(30)$ and the basicity of solvent (DN) act in opposite directions. Deviations from linearity are noted in both polar and nonpolar solvents. The best correlation was obtained by using the Taft multiparameter approach. Fig. 6 *B* shows the fit to the three Taft parameters: π^*, which is a measure for solvent polarity; α, which is a measure for solvent acidity; and β, which is a measure for solvent basicity. The best correlation is

$$\bar{\tau} = 0.272\pi^* + 10.53\alpha - 12.58\beta + 4.086$$

with a noticeable improvement in the correlation ($R = 0.998$). From the relative weight of the three solvent parameters, one can conclude that solvent polarity plays a minor role in the solvation of PNU145156E. On the contrary, solvent basicity and acidity play the major part and are almost equally important. In both the Krigowski and Fawcett and Taft treatments, $\bar{\tau}$ decreases with increasing solvent basicity and increases with increasing solvent acidity. $\bar{\tau}$, measured in solutions containing 50/50% and 80/20% (v/v) dioxane/water, are also shown, in Fig. 6, *A* and *B*. Finally, we placed the measured $\bar{\tau}$ of the PNU145156E:bFGF com-

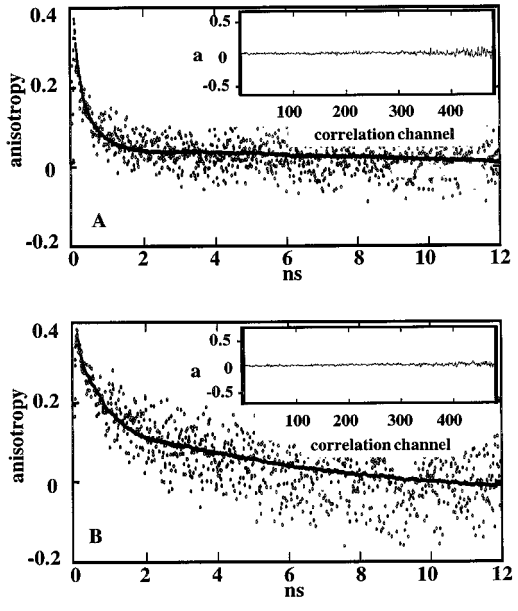

FIGURE 3 Time-resolved fluorescence anisotropy decay of 2.15 μM PNU145156E in PBS (pH 7.1) at 20°C: (*A*) in the absence and (*B*) in the presence of 9.79 μM bFGF. The solid line represents the global analysis fit. The respective autocorrelation functions are shown in the insets.

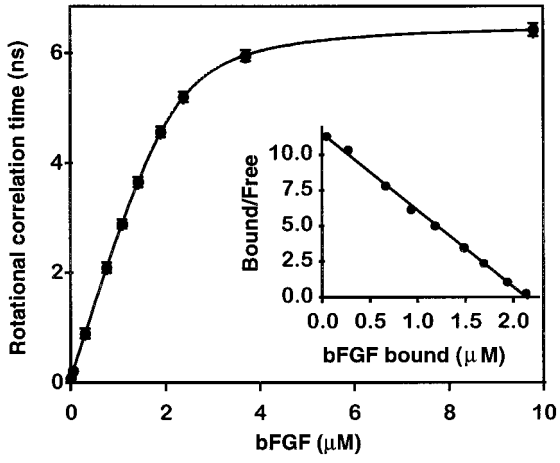

FIGURE 4 Binding of PNU145156E to bFGF, in PBS (pH 7.1) at 20°C, as monitored by time-resolved fluorescence anisotropy titration. The fluorophore concentration was 2.15 μM, and the bFGF concentration was varied from 0.05 μM to 9.79 μM. Rotational correlation times (ϕ) versus bFGF concentration are plotted. The best nonlinear least-squares fit is represented by the solid line. The average of duplicate runs is shown, and each point has a variance of 4% or less. (*Inset*) Scatchard plot.

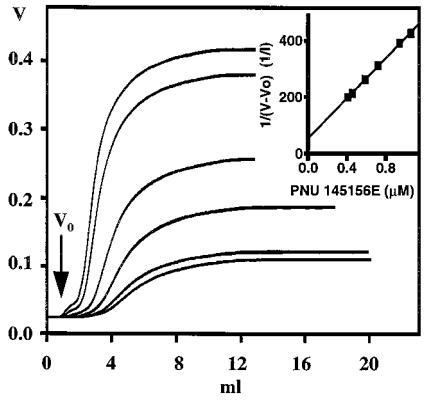

FIGURE 5 Frontal elution of PNU145156E on the 0.64-ml bed volume bFGF column. The following concentrations (in μM) are overlaid: 1.058, 0.939, 0.719, 0.586, 0.446, 0.410. All elution profiles were recorded up to binding site saturation (plateau). (*Inset*) Analysis of elution volumes according to Eq. 2.

plex on the determined linear correlation (*protein* in Fig. 6, *A* and *B*). The local environment of the protein is relatively nonpolar, similar to the isopropanol environment.

PNU145156E steady-state fluorescence anisotropy: effect of chemical modification of bFGF

PNU145156E was titrated by using either bFGF or carboxymethylated bFGF (Cm-FGF) (Caccia et al., 1992; Zamai et al., 1997). The carboxymethylation was at Cys^{69} and Cys^{87}. Saturable binding was measured by steady-state fluorescence anisotropy of the drug (r) as a function of concentration of both the native and the carboxymethylated proteins (Fig. 7). Fitting was carried out according to Eq. 1. In this case, A is r; A_{min} and A_{max} are the anisotropy values of free (r_F) and bound (r_B) drug, respectively (see Materials and Methods). The apparent dissociation constant of PNU145156E:Cm-FGF complex ($K_d^{app} = 8.6 \pm 0.7$ μM) was found to be ~12 times less favorable than the one of PNU145156E:bFGF complex ($K_d^{app} = 0.72 \pm 0.07$ μM). The results indicate that the chemical modification of Cys^{69} and Cys^{87} considerably affects the interaction of the protein with the drug. This conclusion is sustained by two facts: 1) the 3D x-ray structures of Cm-FGF and bFGF are identical (data not shown), and 2) the lifetime varied by no more than 36% for the drug bound to the native protein.

DISCUSSION

Drugs that are capable of inhibiting tumor angiogenesis are becoming increasingly important for therapy against solid tumors. A few in vivo angiogenesis inhibitors have been characterized, but their putative mechanisms of action have not been completely clarified (Terano et al., 1993; Seed, 1996).

In the past few years, a novel class of low toxic angiogenesis inhibitors, named naphthalene sulfonic distamycin A derivatives, have been synthesized and characterized as antitumor agents (Biasoli et al., 1993; Ciomei et al., 1993; Sola et al., 1995). Our research was directed toward better understanding the interaction of PNU145156E with bFGF, which had been inferred from previous in vitro observations (Ciomei et al., 1993; Zamai et al., 1997). We determined the affinity and reversibility of the binding and the stoichiometry of the complex. In addition, the tightness and the forces involved in the complex were sought. The major compound of this family, PNU145156E, is a slightly fluorescent symmetrical polysulfonated naphthylurea with a structure resembling that of suramin (Scheme 1). Unlike the fluorescence of suramin, which increases drastically upon interaction with bFGF (Middaugh et al., 1992), the fluorescence intensity of PNU145156E is unchanged, even in the presence of a 30-fold excess of the protein (Zamai et al., 1997). Data from fluorescence lifetime, anisotropy decay, and QHPAC confirm the formation of a tight PNU145156E:bFGF complex (Table 1). The K_d values obtained by the three different methodologies are similar. Lifetime titration experiments led to $K_d = 145 \pm 5$ nM. Anisotropy decay studies resulted in a somewhat higher K_d (174 ± 4 nM). This is most probably due to the higher drug concentration (~15-fold higher than K_d) required for these measurements. The interaction in a heterogeneous phase between drug and immobilized bFGF yielded $K_d = 150 \pm 7$ nM.

bFGF, with its 146 amino acids, has a single Trp^{114} residue that is located in a region adjacent to the binding cleft. There are seven Tyr residues located at the 24, 73, 103, 106, 111, 115, and 124 amino acid positions in the sequence; only one of them, Tyr^{124}, is expected to be affected by the binding of bFGF to the drug. Preliminary steady-state fluorescence quenching experiments on Trp and Tyr resulted in dissociation constants similar to those obtained by the three independent methods shown in Table 1. The corresponding Stern-Volmer plots, together with time-resolved fluorescence anisotropy studies, will be reported elsewhere.

The high value of the free energy of interaction, ΔG, indicates a very strong interaction between the two components of the complex. Despite this tightness, binding was found to be reversible. The linearity of Scatchard analyses (*insets* of Figs. 2 and 4) suggests a 1:1 binding stoichiometry. Furthermore, the rotational correlation time allowed the determination of displaced volume of the PNU145156E:bFGF complex. Assuming a spherical rotor, the expression for the rotational diffusion coefficient is

$$D_s = k_B T/6V\eta \quad (5)$$

and the rotational correlation time ϕ is related to the rotational diffusion coefficient, D_s, by

$$\phi = 1/6D_s \quad (6)$$

where k_B is the Boltzmann constant, T is the absolute temperature (293 K), V is the displaced volume of the rotor,

TABLE 2 Normalized lifetimes of PNU145156E in different solvents

Solvent	$\bar{\tau}$* (ns)	α_1	τ_1 (ns)	α_2	τ_2 (ns)	χ^2
Water	11.160	0.761	0.630	0.239	11.160	1.22
Methanol	7.460	0.828	0.484	0.172	10.366	1.33
Ethanol	3.727	0.908	0.372	0.092	9.683	1.42
(iso)-Propanol	0.967	0.945	0.496	0.055	4.204	1.41
Acetonitrile	2.901	0.926	0.424	0.074	9.370	1.44
Dioxane 1,4	0.377	0.971	0.395	0.029	3.106	1.26
Dioxane 1,4/water 80/20	2.693	0.933	0.375	0.067	9.607	1.21
Dioxane 1,4/water 50/50	5.658	0.866	0.714	0.134	10.092	1.41
Protein#	1.326	0.955	0.600	0.045	7.044	1.51
PBS	11.140	0.752	0.650	0.248	10.740	1.05

*$\bar{\tau} = \tau_2\alpha_2/\alpha_2^{H_2O}$.
#Protein concentration = 3.96 μM.

and η is the viscosity (~1.02 cP). The displaced volume, calculated from the rotational correlation time of the complex, ϕ_B, is $V = 26{,}018$ Å^3. The radius of the complex is $r = 18.4$ Å. Computer-aided modeling of the PNU145156E:bFGF complex revealed that the calculated rotational correlation time fits a rotating sphere that should be ~15% hydrated, approximating a 1:1 stoichiometry.

The 1:1 complex thus formed exhibits a tight fit between the protein docking region and the corresponding predesigned drug. This is evident from the successful fluorescence lifetime analysis of the PNU145156E:bFGF complex that is based on merely two descret lifetimes. The strong dependence of ($\bar{\tau}$) of PNU145156E on the media (Table 2) could have called for a distribution of lifetimes in a nontight "breathing" complex in which PNU145156E senses multiple nonhomogeneous binding interactions. However, a two-Lorentzian distribution (Global Analysis Package, ISS) did not improve the quality of the lifetime analysis, clearly indicating a tight, homogeneous complex formation.

PNU145156E fluorescence lifetime decay was studied in different solvents to characterize the solvation effect and to gain insight into the nature of the forces involved in its binding with the protein. Such information on the microen-

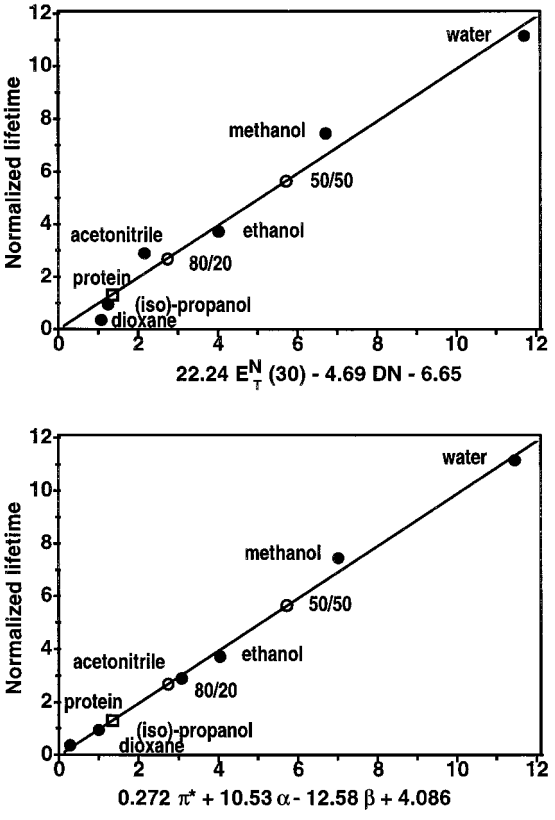

FIGURE 6 (*A*) Correlation between normalized lifetime of PNU145156E $\bar{\tau}_f$ and 22.24 $E_T^N(30) - 4.69$ DN $- 6.65$ in dioxane, (iso)-propanol, acetonitrile, ethanol, methanol, and water (●). (*B*) Correlation between normalized lifetime of PNU145156E $\bar{\tau}_f$ and $0.272\pi^* + 10.53\alpha - 12.58\beta + 4.086$ in dioxane, (iso)-propanol, acetonitrile, ethanol, methanol, and water (●). The solid lines depict the best observed correlations: (*A*) $R = 0.988$ and (*B*) $R = 0.998$. Placed on the correlation lines are the measured $\bar{\tau}$ value in the presence of the protein (□) and the $\bar{\tau}$ values in 50/50% and 80/20% (v/v) dioxane/water, respectively (○).

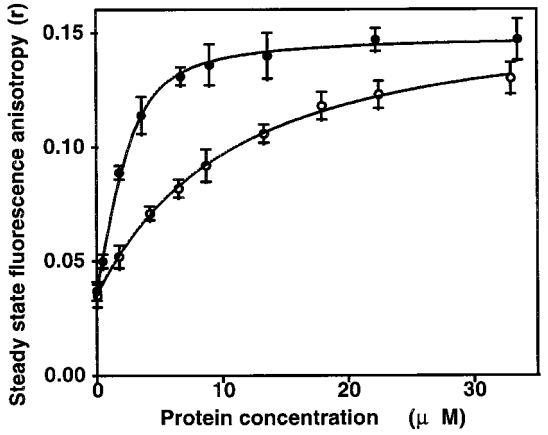

FIGURE 7 Binding of PNU145156E to bFGF and to Cm-FGF, in PBS (pH 7.1) at 20°C, as monitored by steady-state fluorescence anisotropy. The variation of anisotropy, *r*, is plotted versus bFGF (●) or Cm-FGF (○) concentration. The fluorophore concentration was 2.85 μM. The bFGF concentration was varied from 0.49 to 33.5 μM. The Cm-FGF concentration was varied from 0.05 to 32.9 μM. The best nonlinear least-squares fit is represented by the solid line. The average of duplicate runs is shown; each point has a variance of 4% or less.

vironment of the drug, bound to bFGF, is unlikely to be obtained from cocrystallization and x-ray of the PNU145156E:bFGF complex. At the high concentrations needed for cocrystallization (>1 mM), bFGF dimerizes and the drug undergoes self-aggregation (data not shown). This explains the failure to crystallize the 1:1 complex (G. Bolis, personal communication). Therefore, the empirical solvent single-parameter and multiparameter analyses were applied as alternatives. In Fig. 6 *A*, the high values of the positive $E_T^N(30)$ coefficient and the small negative DN basicity coefficient indicate that electrophilic solute/solvent interaction is the dominant solvation mechanism. In Fig. 6 *B*, the high values of α and β coefficients (solvent acidity and basicity) play a major role and are almost equally important in the solvation of PNU145156E. On the contrary, the low value of the π^* coefficient implies that solvent polarity plays a minor role. In both correlations, solvent acidity enhances the relative quantum yield of the long fluorescent component of the drug, whereas solvent basicity has the opposite effect.

Considering the chemical functional groups in PNU145156E (i.e., basicity of the pyrroles and acidity of the sulfonic groups), the resultant analysis agrees with chemical intuition. These analyses enabled us to interpret the observed protein-binding effects on PNU145156E fluorescence by interpolation of the solvation effect, as shown in Fig. 6, *A* and *B*. Clearly, the docking cleft of bFGF is relatively nonpolar, similar to that of isopropanol, yet more polar than that of dioxane. This conclusion is corroborated by $\bar{\tau}$ of PNU145156E in a solution containing 50% water and 50% dioxane by volume. The dielectric constant of this solution is similar to that of acetonitrile, which appears in the lower and less polar part of the correlation shown in Fig. 6. However, $\bar{\tau}$ of the 50:50 water-dioxane solution belongs to the more polar section of the correlation when compared with acetonitrile. This implies that the presence of small quantities of bulk (unbound) water, in an otherwise nonpolar environment, greatly enhances the local polarity of the medium with regard to PNU145156E solvation. Bulk water molecules are thus presumed to be expelled from the contact surface between the drug and the protein, which presumably form a tightly bound complex. Therefore, it is suggested that the drug-binding domain on the protein involves both polar and nonpolar groups that are embedded within a largely hydrophobic core. A delicate balance of all of the different interactions is entailed. The bulk hydrophobic interactions presumably bring together the drug and the protein into a tight complex within a single solvation shell. Furthermore, more specific local interactions, such as hydrogen bonding and acid-base interactions, may account for the additional stability gained in the complex, as evident from the ΔG values.

A "virtual mapping" of the binding sites of the protein can thus be proposed. In the sequence, an assorted pattern of amino acids, which combines specific opposing interactions, is expected. Fig. 8 shows, in the 3D structure of bFGF, a possible path spanning the region from the well-known sulfate-binding site (where Arg^{120} and Lys^{135} are labeled) to a selenate-binding site, as proposed by Eriksson (Eriksson et al., 1993), in the vicinity of Lys^{77} and Glu^{78}. The positive charges at the sulfate- and selenate-binding sites are probably the binding hooks. These two sites of the protein span comparably to the sulfonate groups in the symmetrical naphthalene moieties of PNU145156E. In addition, we have found that the selenate site also includes Cys^{87}, one of the two residues carboxymethylated in Cm-FGF, whose chemical modification strongly affects the binding of PNU145156E (Fig. 7). In contrast, Cys^{69}, the other carboxymethylated residue in Cm-FGF, is located on the opposite surface of the protein, too far from both sulfate- and selenate-binding sites. This suggests that chemically modified Cys^{87} plays a crucial role in the interaction of the protein with the drug. The path, drawn in Fig. 8 between the

FIGURE 8 Ribbon diagram of the Cα backbone of bFGF (*gray*). Amino acid residues are shown as seen in the x-ray crystal structure of bFGF (Eriksson et al., 1993). bFGF putative binding cleft of PNU145156E, spanning the area from the sulfate to the selenate binding sites, is highlighted. Blue: Basic (positive charged) side chains; red: acidic (negative charged) side chains; green: hydrophobic side chains; yellow: hydrogen bonding making side chains; pink: aromatic side chain. Arg^{120} and Lys^{135} are named in the sulfate-binding site, whereas in the selenate-binding site, Lys^{77}, Glu^{78}, and Cys^{87} are shown.

two hooking sites, describes a cleft on the surface of the protein. Along this cleft, hydrophobic side chains are shown in green, hydrogen bond-forming side chains are in yellow, and an aromatic side chain is in pink. This path could represent the specific local interactions as evidenced by the solvent effect. It is also in agreement with previous studies describing the interaction of heparin fragments with bFGF mutants (Thompson et al., 1994).

The particular balance among the various forces involved in PNU145156E:bFGF complex accounts for a mode of interaction different from that of suramin and heparin. On one hand, suramin, in which benzene rings substitute for pyrroles, is a common chaotropic agent. It provokes an extensive and irreversible protein aggregation with a stoichiometry depending on drug concentration (Middaugh et al., 1992). This can explain the drug side effects observed in vivo. On the other hand, the interaction with heparin and heparin fragments (polysulfate-polysaccharide) induces the dimerization of bFGF (Klagsbrun and Baird, 1991), forming a complex with a 1:2 stoichiometry (Ornitz et al., 1992; Thompson et al., 1994). It is this trimeric complex that positively modulates the binding of bFGF to its receptor (Yayon et al., 1991; Aviezer et al., 1994), resulting in the activation of the angiogenesis process. Unlike chaotropic agents, PNU145156E seems to be more specific for bFGF. The binding to the protein is driven by the combined hydrophobic and hydrogen bonding acceptor sites of the pyrrole backbone. It is further strengthened by local and specific interaction of sulfonic charged groups. The advantage of the proposed binding model lies in the specificity of the interactions involved. Specificity is demonstrated not only by the solvent effect, but also by the studies of point chemical modification. The good tolerability of PNU145156E in vivo might be ascribed to its specific and reversible interaction. Its tight binding to bFGF in a 1:1 complex presumably prevents the formation of the 2:1 complex of bFGF with heparin that is essential for its binding to the receptor, a prerequisite for the activation of the angiogenic process.

In conclusion, this study indicates that PNU145156E forms a tight but reversible complex with bFGF. It is most likely that this interaction covers a large surface of the protein involving the heparin-binding domain described by Thompson (1994) and the selenate-binding site proposed by Eriksson (1993). Thus this relatively small molecule, forming a 1:1 complex with bFGF, is able to prevent biologically effective dimerization of bFGF.

We are most grateful for the technical help of Mrs. Batia Uzan and Dr. I. Fishov. We thank Prof. F. Kezdy, Prof. D. Gill, and Dr. M. Grandi for their suggestions and critical review, Dr. G. Bolis and Dr. A. Vulpetti for discussing x-ray and modeling data, and Dr. R. Cohen-Luria for help in manuscript preparation.

The financial support from ONR grant N00014-96-1-80 and the Israel Academy of Sciences and Humanities Grant 348/91 is gratefully acknowledged.

This paper was in partial fulfillment of a Ph.D. thesis by MZ.

REFERENCES

Abraham, M. H., P. L. Greller, J. M. Abboud, R. M. Doherty, and R. W. Taft. 1988. Solvent effects in organic chemistry—recent developments. *Can. J. Chem.* 66:2673–2686 and references therein.

Alfahel, A., A. Korngreen, A. H. Parola, and Z. Priel. 1996. Purinergically induced membrane fluidization in ciliary cells: characterization and control by calcium and membrane potential. *Biophys. J.* 70:1045–1053.

Auerbach, W., and R. Auerbach. 1994. Angiogenesis inhibitors: a review. *Pharmacol. Ther.* 63:265–311.

Aviezer, D., E. Levy, M. Safran, C. Svahn, E. Buddecke, A. Schmidt, G. David, I. Vlodavsky, and A. Yayon. 1994. Differential structural requirements of heparin and heparan sulfate proteoglycans that promote binding of basic fibroblast growth factor to its receptor. *J. Biol. Chem.* 269:114–121.

Baird, A., D. Schubert, N. Ling, and R. Guillemin. 1988. Receptor- and heparin-binding domains of basic fibroblast growth factor. *Proc. Natl. Acad. Sci. USA.* 85:2324–2328.

Basilico, C., and D. Moscatelli. 1992. The FGF family of growth factors and oncogenes. *Adv. Cancer Res.* 59:115–165.

Biasoli, G., M. Botta, M. Ciomei, F. Corelli, M. Grandi, F. Manetti, N. Mongelli, and A. Paio. 1993. New heterocyclic analogs of suramin with bFGF inhibiting activity. Synthesis, sar and possible mode of action. *Med. Chem. Res.* 4:202–210.

Blood, C. H., and B. R. Zetter. 1990. Tumor interaction with the vasculature: angiogenesis and tumor metastasis. *Biochim. Biophys. Acta.* 1032:89–118.

Burgess, W. H., and T. Maciag. 1989. The heparin-binding (fibroblast) growth factor family of proteins. *Annu. Rev. Biochem.* 58:575–606.

Burke, T. G., and Z. Mi. 1994. The structural basis of camptothecin interactions with human serum albumin: impact on drug stability. *J. Med. Chem.* 37:40–46.

Caccia, P., G. Nitti, O. Cletini, P. Pucci, M. Ruoppolo, F. Bertolero, B. Valsasina, F. Roletto, C. Cristiani, G. Cauet, P Sarmientos, A. Malorni, and G. Marino. 1992. Stabilization of recombinant human basic fibroblast growth factor by chemical modifications of cysteine residues. *Eur. J. Biochem.* 204:649–655.

Ciomei, M., W. Pastori, M. Mariani, F. Sola, M. Grandi, N. Mongelli. 1993. New sulfonated distamycin A derivatives with bFGF complexing activity. *Biochem. Pharmacol.* 47:295–302.

Eriksson, A. E., L. S. Cousens, and B. W. Matthews. 1993. Refinement of the structure of human basic fibroblast growth factor at 1.6 Å resolution and analysis of presumed heparin binding sites by selenate substitution. *Protein Sci.* 2:1274–1284.

Faham, S., R. E. Hileman, J. R. Fromm, R. J. Linhardt, and D. C. Rees. 1996. Heparin structure and interactions with basic fibroblast growth factor. *Science.* 271:1116–1120.

Fassina, G., and I. M. Chaiken. 1987. Analytical high performance affinity chromatography. *In* Advances in Chromatography, Vol. 27. J. C. Giddings, E. Grushka, and P. R. Brown, editors. Marcel Dekker, New York and Basel. 247–297.

Fernig, D. G., and J. T. Gallagher. 1994. Fibroblast growth factors and their receptors: an information network controlling tissue growth, morphogenesis and repair. *Prog. Growth Factor Res.* 5:353–377.

Folkman, J. 1971. Tumor angiogenesis: therapeutic implications. *N. Engl. J. Med.* 285:1182–1186.

Folkman, J. 1985. Tumor angiogenesis. *Adv. Cancer Res.* 43:175–203.

Folkman, J., and M. Klagsbrun. 1987. Angiogenetic factors. *Science.* 235:442–447.

Glikberg, S., and Y. Markus. 1983. Relation of the Gibbs free energy of transfer of ions from water to polar solvents to the properties of the solvents and the ions. *J. Solution Chem.* 12:255–270.

Gullino, P. M. 1978. Angiogenesis and oncogenesis. *J. Natl. Cancer Inst.* 61:639–643.

Gutmann, V. 1968. Coordination Chemistry in Non-aqueous Solvents. Springer Verlag, Vienna and New York.

Hazan, S., I. Fishov, M. Zamai, V. R. Caiolfa, and A. H. Parola. 1995. Fluorescence polarization assay for endothelin converting enzymes. *Peptides.* 60:333–336.

Herblin, W. F., S. Brem, T. P. Fan, and J. L. Gross. 1994. Recent advances in angiogenesis inhibitors. *Exp. Opin. Ther. Patents.* 4:641–654.

Hulme, E. C., and N. J. M. Birdsall. 1992. Strategy and tactics in receptor-binding studies. *In* Receptor-Ligand Interactions. A Practical Approach. E. C. Hulme, editor. Oxford University Press, New York. 63–176.

Klagsbrun, M., and A. Baird. 1991. A dual receptor system is required for basic fibroblast growth factor activity. *Cell.* 67:229–231.

Klagsbrun, M., and P. A. D'Amore. 1991. Regulators of angiogenesis. *Annu. Rev. Physiol.* 53:17–39.

Kohler, K., J. Trepel, and W. Linehan. 1992. Suramin: a novel growth factor antagonist with activity in hormone-refractory metastatic cancer. *J. Clin. Oncol.* 10:881–889.

Kosower, E. M. 1968. An Introduction to Physical Organic Chemistry. Wiley, New York. 293.

Krygowski, T. M., and W. R. Fawcett. 1975. Complementary Lewis acid-base description of solvent effects. I. Ion-ion and ion-dipole interactions. *J. Am. Chem. Soc.* 97:2143–2148.

La Rocca, R. V., C. A. Stein, and C. E. Meyers. 1990. Suramin: prototype of a new generation of antitumor compounds. *Cancer Cell.* 2:106–115.

Lindahl, U., K. Lidholt, D. Spillmann, and L. Kjellen. 1994. More to heparin than anticoagulation. *Thromb. Res.* 75:1–32.

Liotta, L. A., P. S. Steeg, and W. G. Stetler-Stevenson. 1991. Cancer metastasis and angiogenesis: an imbalance of positive and negative regulation. *Cell.* 64:327–336.

Middaugh, C. R., H. Mach, C. J. Burke, D. B. Volking, J. M. Dabora, P. K. Tsai, M. W. Bruner, J. A. Ryan, and K. E. Marfia. 1992. Nature of the interaction of growth factors with suramin. *Biochemistry.* 31: 9016–9024.

Ornitz, D. M., A. B. Herr, M. Nilsson, J. Westman, C. M. Svahn, and G. Waksman. 1995. FGF binding and FGF receptor activation by synthetic heparan-derived di- and trisaccharides. *Science.* 268:432–436.

Ornitz, D. M., A. Yayon, J. G. Flanagan, C. M. Svahn, E. Levi, E., and P. Leder. 1992. Cell surface, heparin-like molecules are required for binding of basic fibroblast growth factor to its high affinity receptor. *Mol. Cell. Biol.* 12:240–247.

Presta, M., M. Rusnati, A. Gualandris, P. Dell'Era, C. Urbinati, D. Coltrini, E. Tanghetti, and M. Belleri. 1994. Human basic fibroblast growth factor: structure-function relationship of an angiogeneic molecule. *In* Angiogenesis: Molecular Biology, Clinical Aspects. Series A: Life Sciences. 263. M. E. Maragoudakis, P. M. Gullino, and P. I. Lelkes, editors. Plenum Press, New York. 39–50.

Reichardt, C. 1990. Solvent and Solvent Effects in Organic Chemistry. VCH, Weinhein, Germany.

Reichardt, C. 1994. "Solvatocromic dyes" as solvent polarity indicators. *Chem. Rev.* 94:2319–2358.

Seed, M. P. 1996. Angiogenesis inhibition as a drug target for diseases: an update. *Exp. Opin. Invest. Drugs.* 5:1617–1637.

Sola, F., M. Farao, E. Pesenti, A. Marsilio, N. Mongelli, and M. Grandi. 1995. Antitumoral activity of FCE26644, a new growth-factor complexing molecule. *Cancer Chemother. Pharmacol.* 36:217–222.

Springer, B. A., M. W. Pantoliano, F. A. Barbera, P. L. Gunyuzlu, L. D. Thompson, W. F. Herblin, S. A. Rosenfeld, and G. W. Book. 1994. Identification and concerted function of two receptor binding surfaces on basic fibroblast growth factor required for mitogenesis. *J. Biol. Chem.* 269:26869–26884.

Terano, H., Y. Shibata, and T. Otsuka. 1993. Angiogenesis inhibitors of microbial origin. *Drugs Future.* 18:239–247.

Thompson, L. D., M. W. Pantoliano, and B. A. Springer. 1994. Energetic characterization of the basic fibroblast growth factor-heparin interaction: identification of the heparin binding domain. *Biochemistry.* 33: 3831–3840.

Vlodavsky, I., R. Bar-Shavit, R. Ishai-Michaeli, P. Bashkin, and Z. Fuks. 1991. Extracellular sequestration and release of fibroblast growth factor: a regulatory mechanism. *Trends Biochem. Sci.* 16:268–271.

Yayon, A., M. Klagsbrun, J. D. Esko, P. Leder, and D. M. Ornitz. 1991. Cell surface, heparin-like molecules are required for binding of basic fibroblast growth factor to its high affinity receptor. *Cell.* 64:841–848.

Zamai, M., and G. Fassina. 1991. Mobile phase effects in the high-performance affinity purification of thermolysin. *J. Chromatogr.* 549: 195–205.

Zamai, M., A. H. Parola, N. Mongelli, M. Grandi, and V. R. Caiolfa. 1997. Naphthalene sulfonic distamycin-A derivatives: interaction with human basic fibroblast growth factor. *Med. Chem. Res.* 7:36–44.

Zhong-yuan, Z., S. Cheng-e, and H. Te-kang. 1985. Solvent effects on the rate of the reaction of 2,4-dinitrofluorobenzene with the ethyl ester of tyrosine. *J. Chem. Soc. Perkin Trans.* 11:929–934.

Zhu, H., K. Ramnarayan, J. Anchin, W. Y. Miao, A. Sereno, L. Millman, J. Zheng, V. N. Balaji, and M. E. Wolff. 1995. Glu-96 of basic fibroblast growth factor is essential for high affinity receptor binding. *J. Biol. Chem.* 270:21869–21874.

Zhu, X., H. Komiya, A. Chirino, S. Faham, G. M. Fox, T. Arakawa, B. T. Hsu, and D. C. Rees. 1990. Three-dimensional structure of acidic and basic fibroblast growth factors. *Science.* 251:90–93.